



Equilibrium of Methane and Carbon Dioxide Hydrates Below the Freezing Point of Water: Literature Review and Modeling

Ehsan Heidaryan^{1,2} · Maria Dolores Robustillo Fuentes² · Pedro de Alcântara Pessôa Filho²

Received: 9 July 2018 / Accepted: 31 July 2018 / Published online: 11 August 2018
© Springer Science+Business Media, LLC, part of Springer Nature 2018

Abstract

This work presents a review of literature data of methane and carbon dioxide hydrate equilibrium at low temperatures. Constants of Arrhenius-type equation accurately determined for the mentioned lines which allow calculating the hydrate equilibrium pressure at any temperature below the quadruple point for both systems contain ice or supercooled water. Through intersection analysis, new accurate quadruple points were determined. Interpretations based on flash calculations by high accurate equations of states shown enthalpies of clathrate formation/dissociation, for equilibrium below quadruple point, lead to the similarity of Clapeyron and Clausius–Clapeyron approaches. Based on equality of equilibrium conditions at the quadruple point, new hydration numbers were calculated. Gamma–phi approach through high accurate equations of states of GERG-2008 and CG for the prediction of VHIw three-phase equilibrium line was evaluated. Commercial packages of Multiflash and PVTsim and open-source codes of CSMGem and CSMHYD were used to model the phenomena.

Keywords Methane · Carbon dioxide · Hydrate · Low temperatures

✉ Ehsan Heidaryan
e.heidaryan17@imperial.ac.uk; heidaryan@engineer.com
Pedro de Alcântara Pessôa Filho
pedropessoa@usp.br

¹ Department of Chemical Engineering, Imperial College London, South Kensington Campus, London SW7 2AZ, UK

² Department of Chemical Engineering, Engineering School, University of São Paulo (USP), Caixa Postal 61548, São Paulo, SP 05424-970, Brazil

1 Introduction

Hydrates are solid crystalline compounds formed by the inclusion of a guest molecule inside a cavity formed by water molecules structured in a hydrogen-bond network [1]. These compounds are also known as clathrates [2].

Hydrates occur naturally beneath the permafrost in polar regions and in marine sediments and contain large amounts of untapped gases. The main gas component of these hydrates is methane, but small amounts of heavier hydrocarbons, carbon dioxide and hydrogen sulfide have also been recovered [3, 4]. Hydrates are also known to occur at and near the surface of Mars [5, 6]. While methane is the most common guest compound in hydrates, carbon dioxide is also an important hydrate-forming gas [7–9].

Hydrates may provide a safe way to transport gases. The capital cost for natural gas hydrate transportation facilities is lower than for liquefied natural gas (LNG), an established method [10]. The production of methane from natural gas hydrates is expected to have a far higher impact on the global economy than the impact of shale [11]. Finally, atmospheric methane concentrations have undergone significant changes in the past, and it is widely accepted that these have occurred in conjunction with shifts in global climate [12]. Current studies indicate a need for an abatement strategy to reduce emissions from thawing permafrost. An aggressive abatement policy, in addition to other benefits, will reduce the mean extra impacts of emissions from thawing permafrost by about US\$ 37–50 trillion [13].

This work presents a literature review of experimental data of equilibrium pressure of single guest hydrates of methane and carbon dioxide at temperatures below the quadruple point. The experimental data on vapor + hydrate + water – ice (VHIw) three-phase equilibrium were modeled through a gamma–phi (γ – ϕ) approach. This approach comprises the van der Waals and Platteeuw [14] adsorption theory, without mutual interaction of the adsorbed guest molecules according to Ballard and Sloan [15], coupled with the highly accurate equations of states GERG-2008 [16] and its extension for carbon capture and storage (CCS) process EOS-CG [17]. The commercial phase equilibrium packages PVTsim [18] and Multiflash [19] and the open-source packages CSMGem [20] and CSMHYD [21] were also considered for comparison. Finally, the three-phase equilibrium line of VHIw was correlated by an Arrhenius-type equation [22] coupled with the Clapeyron [23] equation. By considering the Clausius–Clapeyron [24] equation, the enthalpy of hydrate formation/dissociation was calculated. The quadrupole points and the hydration numbers estimated by this approach are in good agreement with other approaches.

2 Literature Review

2.1 Experimental Data

2.1.1 Methane

Details of experimental literature data for methane hydrate below the freezing point of water [25–35], the uncertainties in their measurements and the purity of the compounds used in the experiments are presented in Table 1. Figure 1 presents an overview of

Table 1 Details of experimental literature data for methane hydrate equilibrium at low temperatures

Author/reference	Year	Data points	$\Delta(T)$ (K)	$u(P)$ (kPa)	$u(T)$ (K)	Methane purity (%)	Quality of water
Roberts et al. [25]	1940	1	259	n.a.	n.a.	n.a.	n.a.
Deaton and Frost [26]	1946	5	262.4–270.9	13.8	0.03	99.7	Distilled
Delsemme and Wenger [27]	1970	8	82–100	0.01	n.a.	n.a.	n.a.
Falabella and Vanpee [28]	1974	5	148.8–191.3	6.5	0.05	99.97	n.a.
Makogon and Sloan [29]	1994	6	190.15–262.4	n.a.	0.1	99.9	n.a.
Yang [30]	2000	1	259.1	n.a.	n.a.	n.a.	n.a.
Hachikubo et al. [31]	2002	4	268.4–271.28	n.a.	n.a.	n.a.	n.a.
Yasuda and Ohmura [32]	2008	11	244.2–272.2	20	0.2	99.99	Distilled/detonized
Mohammadi and Richon [33]	2010	4	263.2–272.6	5	0.1	99.995	Distilled/detonized
Fray et al. [34]	2010	6	145.75–195.74	1.2	0.05	n.a.	n.a.
Nagashima and Ohmura [35]	2016	7	197.3–238.7	1.8	0.15	99.99	Distilled

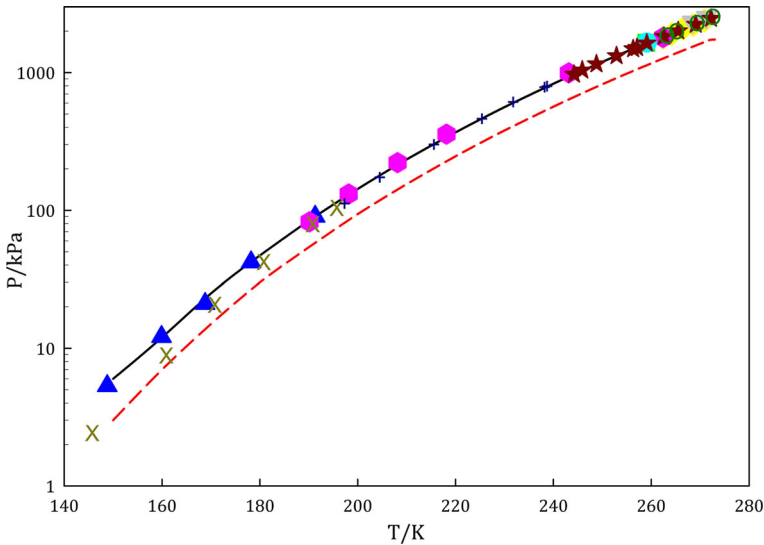


Fig. 1 Overview of literature experimental data for equilibrium conditions for methane, hydrate and ice at temperatures below the quadrupole point. (Istomin et al. [36] hexagonal ice: continuous line; Istomin et al. [36] cubic ice: dashed line; Roberts et al. [25]: filled square; Deaton and Frost [26]: filled diamond; Falabella and Vanpee [28]: filled upward triangle; Makogon and Sloan [29]: empty square; Yang [30]: filled circle; Hachikubo et al. [31]: filled downward triangle; Yasuda and Ohmura [32]: filled star; Mohammadi and Richon [33]: empty circle; Fray et al. [34]: cross symbol; Nagashima Ohmura [35]: plus symbol) (Color figure online)

these data. The experimental data obtained by Delsemme and Wenger [27] are not presented due to very low temperature and pressure range of that data set.

The trend presented by the experimental data is overall the same, but some discrepancies are observed for the results by Fray et al. [34] at low temperatures. Figure 1 also presents the results by Istomin et al. [36] for molecular dynamic (MD) simulations for both hexagonal and cubic ice. For the same temperature, the equilibrium pressure is lower with cubic ice. A likely explanation for the discrepancy observed by Fray et al. [34] is the formation of cubic ice at lower temperatures. The possibility of hydrate equilibrium with supercooled water for methane was also presented by Istomin and coworkers [36]. Experimental evidenced for methane hydrate in equilibrium with supercooled water was investigated by Melnikov et al. [37]. Their results are presented in Fig. 2 and compared with molecular dynamics simulations by Istomin et al. [36].

2.1.2 Carbon Dioxide

An outline of the existing data sets for carbon dioxide hydrate formation below the freezing point of water is presented in Table 2 [31, 32, 34, 38–45]. This table also presents information concerning measurement uncertainties in temperature and pressure or on the purity of the carbon dioxide and water used, when available.

Figure 3a presents an overview of these literature data. The trend presented by the experimental data is overall the same. Figure 3a also presents the results of Istomin and coworkers [36]. Their results indicate that all experimental data sets were obtained for

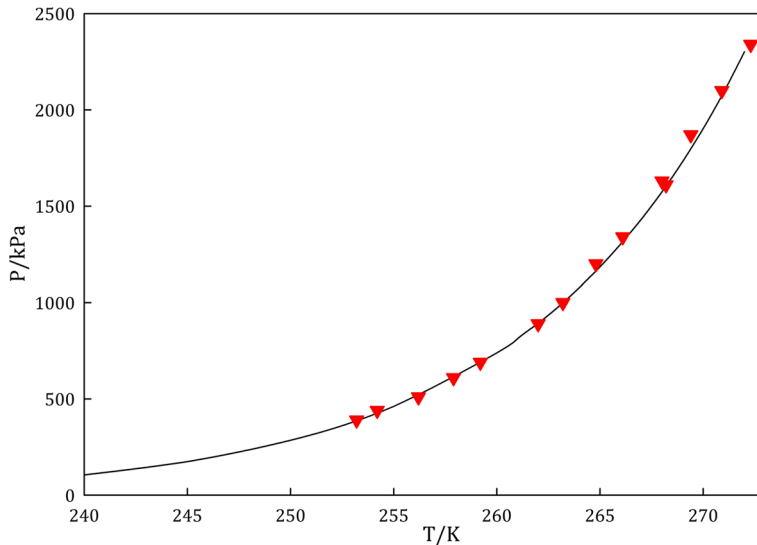


Fig. 2 Overview of literature experimental data for equilibrium conditions for methane, hydrate and supercooled water at temperatures below the quadrupole point. (Istomin et al. [36] supercooled water: continuous line; Melnikov et al. [37]: filled downward triangle) (Color figure online)

hexagonal ice: The equilibrium with cubic ice system would occur only at pressures roughly at 33% lower pressure. Figure 3b presents a magnification of the experimental data close to the quadrupole point. It shows that the molecular dynamic simulations by Istomin et al. [36] for systems containing hexagonal ice agree with the experimental data by Larson [38], but underestimates the equilibrium pressure of the other data sets.

The results by Istomin et al. [36] for carbon dioxide hydrate equilibrium with supercooled water are presented in Fig. 4, along with the experimental data by Melnikov et al. [46] and Nema et al. [47]. The concordance between experimental results and simulations is remarkable, even though the equilibrium pressure determined by Nema et al. [47] is slightly higher.

2.2 Phase Equilibrium Modeling

Although new models have been recently proposed to describe gas hydrate equilibrium [48], the most widely used approach is the van der Waals and Platteeuw [14] (vdWP) equation. The vdWP model uses the Langmuir adsorption theory [49] to evaluate the chemical–potential difference of water in the metastable empty hydrate β -lattice and in the hydrate lattice stabilized by the presence of guest molecules. The commercial package Multiflash [19] uses the vdWP model [14] combined to the Cubic-Plus-Association (CPA) Equation of State [50] to predict hydrate phase equilibrium.

The vdWP model may fail when calculating cavity occupancy in multiple occupancy situations [51–53]. This model has undergone several modifications to improve its performance [54–59]. The first important improvement was carried out by Parrish and Prausnitz [54]. These authors used a reference hydrate for which the chemical–potential difference could be determined from available experimental data for

Table 2 Details of experimental literature data for carbon dioxide hydrate equilibrium at low temperatures

Author/Reference	Year	Data points	$\Delta(T)$ (K)	$\mu(P)$ (kPa)	$\mu(T)$ (K)	CO ₂ purity (%)	Quality of water
Larson [38]	1955	10	256.8–271.8	70	0.1	99.9	n.a.
Miller and Smythe [39]	1970	8	151.52–192.54	n.a.	n.a.	n.a.	n.a.
Adamson and Jones [40]	1971	4	196.78–200.96	n.a.	n.a.	n.a.	n.a.
Falabella [41]	1975	4	194.5–218.2	n.a.	0.05	n.a.	n.a.
Schmitt [42]	1986	6	195–213.6	n.a.	n.a.	n.a.	n.a.
Wendland et al. [43]	1999	1	271.14	5	0.05–0.1	99.95	Twice distilled
Hachikubo et al. [31]	2002	6	263.17–271.23	n.a.	n.a.	n.a.	n.a.
Yasuda and Ohmura [32]	2008	10	244.5–269.4	20	0.2	99.995	Distilled/deionized
Mohammadi and Richon [44]	2009	4	264.5–271	5	0.1	99.998	Deionized
Fray et al. [34]	2010	3	172.28–182.36	0.08–0.4	0.02–0.1	99.998	Distilled/deionized
Nagashima et al. [45]	2016	8	199.1–247.1	0.5	0.1	99.995	Distilled/deionized

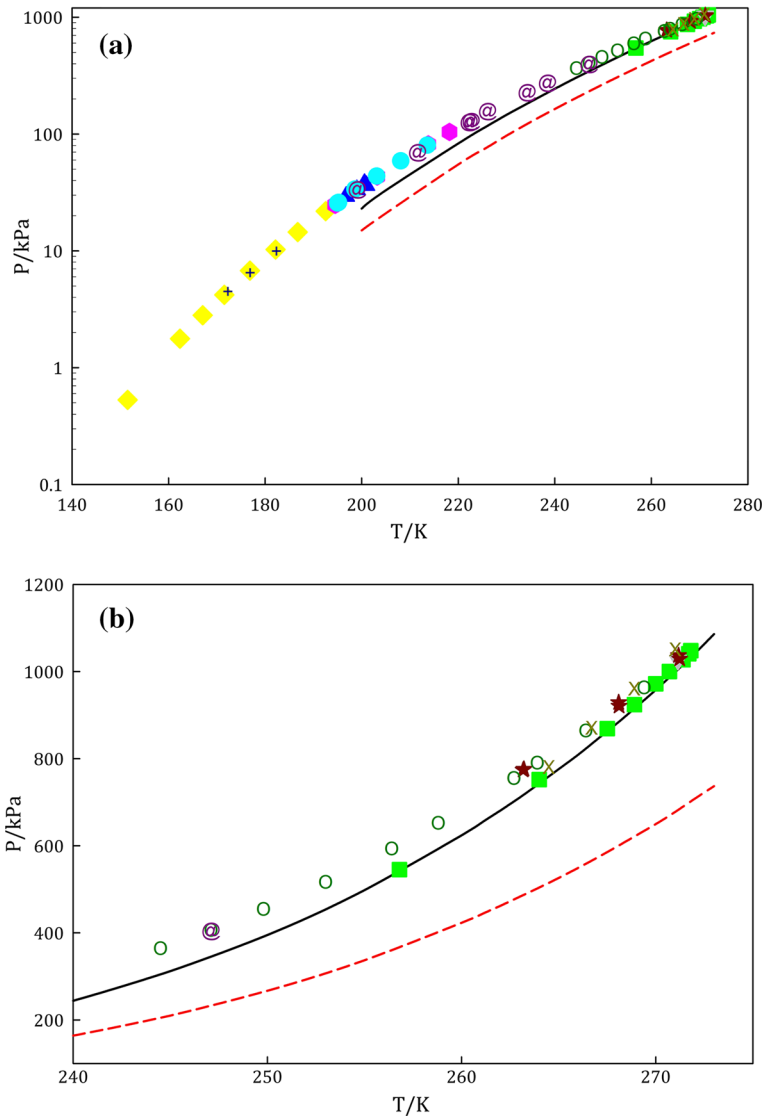


Fig. 3 Literature experimental data for equilibrium conditions for carbon dioxide, hydrate and ice at temperatures below the quadrupole point. **a** overview (Istomin et al. [34] hexagonal ice: continuous line; Istomin et al. [34] cubic ice: dashed line; Larson [38]: filled square; Miller and Smythe [39]: filled diamond; Adamson and Jones [40]: filled upward triangle; Falabella [41]: empty square; Schmitt [42]: filled circle; Wendland et al. [43]: filled downward triangle; Hachikubo et al. [31]: filled star; Yasuda and Ohmura [32]: empty circle; Mohammadi and Richon [44]: cross symbol, Fray et al. [34]: plus symbol; Nagashima et al. [45]: commercial at symbol). **b** magnification close to the quadrupole point: (Istomin et al. [36] hexagonal ice: continuous line; Istomin et al. [36] cubic ice: dashed line; Larson [38]: filled square; Wendland et al. [33]: filled downward triangle; Hachikubo et al. [31]: filled star; Yasuda and Ohmura [32]: empty circle; Mohammadi and Richon [44]: cross symbol; Nagashima et al. [45]: commercial at symbol) (Color figure online)

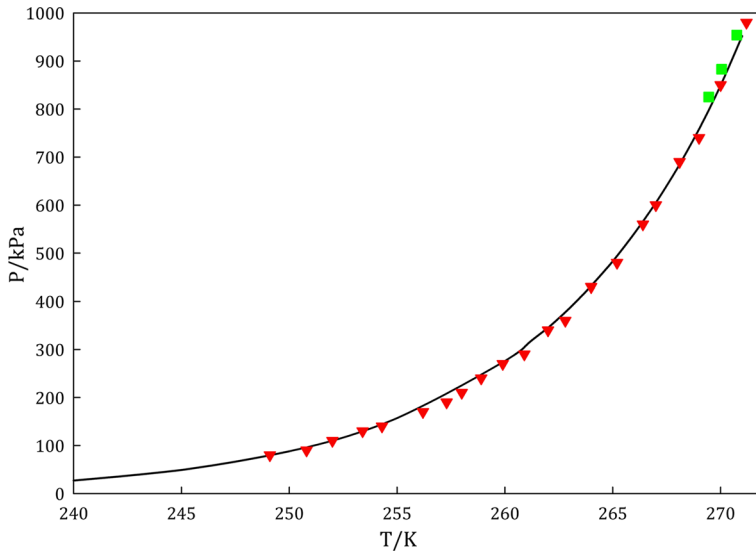


Fig. 4 Overview of experimental literature data for equilibrium conditions for carbon dioxide, hydrate and supercooled water at temperatures below the quadrupole point. (Istomin et al. [36] supercooled water: continuous line; Melnikov et al. [46]: filled downward triangle; Nema et al. [47]: filled square) (Color figure online)

equilibrium at reference conditions. This modification, in combination with the SRK-EOS [60], was used in the CSMHyd code [21] and in PVTsim package [18]. Ballard and Sloan [15] introduced further modifications to improve the performance of the vdWP approach. Their work is the backbone of the CSMGem code [20] for calculating hydrate formation conditions. Vinš and coworkers [61] fitted the parameters of Ballard and Sloan [15] model using highly accurate EOSs [16, 17].

As shown in Figs. 1, 2, 3 and 4, hydrate equilibrium pressures follow a logarithmic trend similar to that presented by the vapor pressures of pure substances. Therefore, representing the natural logarithm of hydrate pressure as a function of the reciprocal of absolute temperature at equilibrium condition may provide an appropriate description for the experimental data. Anderson [62] used a quadratic equation to represent data along the coexistence line (ice, hydrate and vapor) for methane hydrates based on this technique. Furthermore, Anderson [63] correlated the equilibrium line for carbon dioxide hydrate data by Larson [38] using a similar approach with a second-order polynomial fit.

3 Results and Discussion

3.1 Correlation of Experimental Data

Figure 5 shows the hydrate pressure (in logarithm scale) as a function of the reciprocal of temperature along the equilibrium line for ice, methane hydrate and vapor. The linear behavior is apparent.

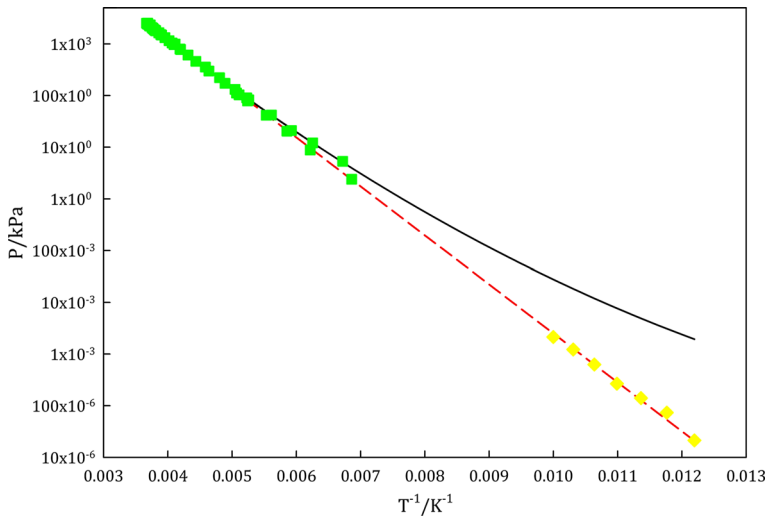


Fig. 5 Hydrate equilibrium pressure as a function of the reciprocal of temperature for methane, ice and hydrate: experimental data and modeling. (Anderson [62]: continuous line; Eq. 1: dashed line; data depicted in Fig. 1: filled square; Delsemme and Wenger [27]: filled diamond) (Color figure online)

Table 3 Parameters A_i for Eqs. (1) and (2)

i	Guest molecule			
	Methane		Carbon dioxide	
	Ice	Supercooled water	Ice	Supercooled water
1	1.58297×10^1	3.18030×10^1	1.63686×10^1	8.86456×10^1
2	-2.18367×10^3	-6.54584×10^3	-2.55918×10^3	-3.54994×10^4
3	–	–	–	3.61428×10^6

The experimental data can be fitted by the following Arrhenius-like equation:

$$\frac{P}{\text{kPa}} = \exp\left(A_1 + \frac{A_2}{(T/K)}\right) \quad (1)$$

The parameters of Eq. 1 fitted to the data in Fig. 5 are presented in Table 3. The data by Delsemme and Wenger [27] were not considered in the fitting: They were considered just to evaluate the extrapolative capability of Eq. (1). The resulting fit is presented in Fig. 5, along with the results for Anderson's [62] quadratic equation. It can be seen that the correlation proposed correlates precisely the experimental data over the entire temperature range, with only two adjustable parameters. Moreover, the extrapolation of Eq. (1) for low temperatures results in a very good prediction of the experimental data.

The same procedure was used to correlate the equilibrium pressures of supercooled water, methane hydrate and methane vapor. The corresponding parameters are also

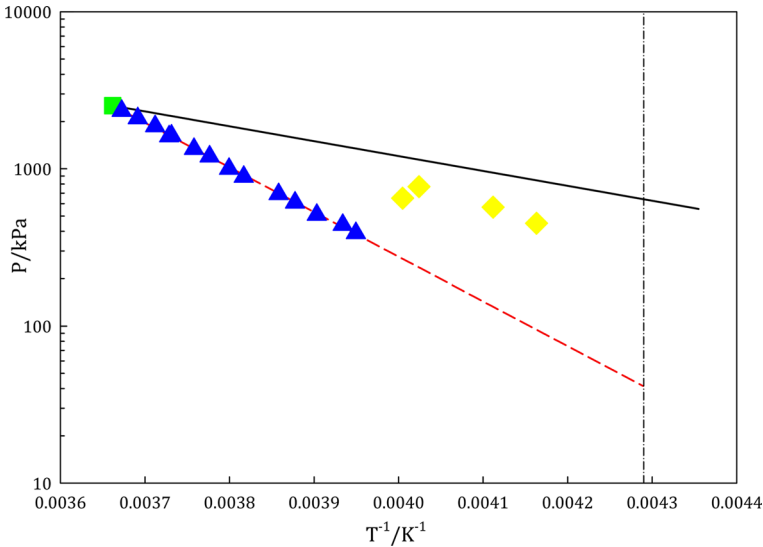


Fig. 6 Hydrate equilibrium pressure as a function of the reciprocal of temperature for methane, supercooled water and hydrate: experimental data and modeling. (Equation 1 (ice): continuous line; Eq. 1 (supercooled water): dashed line; quadruple point: filled square; methane hydrate dissociation ($T < 253$) [37]: filled diamond; methane hydrate dissociation ($T > 253$) [37]: filled upward triangle; supercooled water lower temperature limit: dash-point line) (Color figure online)

presented in Table 3. The performance of Eq. (1) can be seen in Fig. 6. This figure shows how the equilibrium curve with supercooled water deviates from the equilibrium curve with ice. The equilibrium curve with supercooled water can be extended down to 233.15 K, which is the minimum temperature in which supercooled water exists [64]. Melnikov et al. [46] obtained experimental equilibrium conditions close to this limit. These data were not considered in the modeling, but are presented in Fig. 6. In this case, the experimental uncertainty is a high cue to the small hydrate samples, and the experimental data follow a different trend from data at higher temperatures.

The intersection between the curves for the equilibrium with either ice and supercooled water is the quadrupole point. The calculated quadrupole point, considering Eq. (1) for both equilibria, is 273.09 K and 2523.79 kPa. These values are in very good agreement with the values reported by Selim and Sloan [65].

Figure 7 presents the equilibrium pressure (in logarithm scale) for ice, carbon dioxide and hydrate. A trend similar to that for the equilibrium with ice, methane and hydrate is observed.

The values of the parameters of Eq. (1) fitted to the experimental data are presented in Table 3. Figure 7 presents the results from the fitting of Eq. (1) to the experimental data. The results obtained by extrapolating the quadratic polynomial fit by Anderson [63] are also presented. That Eq. (1) is suitable to describe this equilibrium is evident from these results. Concerning the polynomial fit by Anderson [63], Fig. 7 underscores the obvious fact that a polynomial correlation cannot be used outside the range of conditions for which the parameters were fitted.

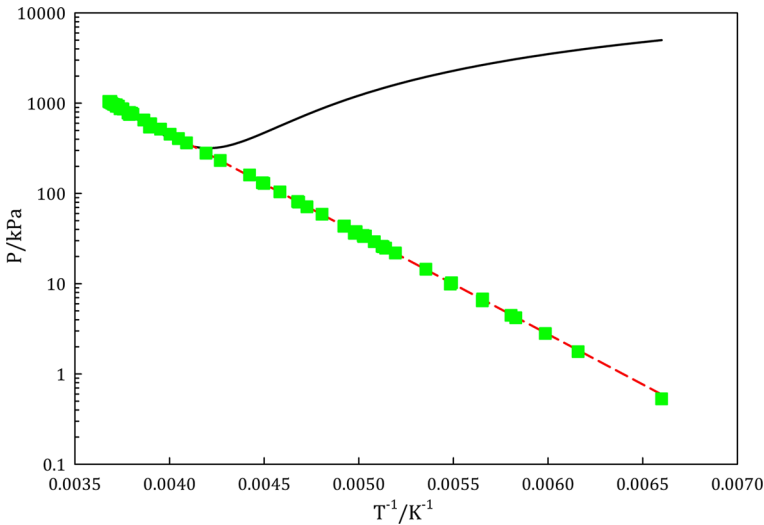


Fig. 7 Hydrate equilibrium pressure as a function of the reciprocal of temperature for carbon dioxide, ice and hydrate: experimental data and modeling. (Anderson [63]: continuous line; Eq. 1: dashed line; data depicted in Fig. 1: filled square) (Color figure online)

For the equilibrium of water/supercooled water, carbon dioxide and hydrate, there is a subtle deviation in the linearity, which makes Eq. (1) unsuitable for the description of this equilibrium. Therefore, the experimental data were fitted using Eq. (2):

$$\frac{P}{\text{kPa}} = \exp\left(A_1 + \frac{A_2}{(T/K)} + \frac{A_3}{(T/K)^2}\right) \quad (2)$$

The values of the parameters of Eq. (2) fitted to the experimental equilibrium data for water/supercooled water, carbon dioxide and hydrate are presented in Table 3. Figure 8 presents the results obtained from this fitting, along with the results obtained by using the equations by Melnikov et al. [46] and Nema et al. [47]. This figure highlights the necessity of adding the parameter A_3 to Eq. (2). While the linear fit of Melnikov et al. [46] cannot predict the high-temperature region, the linear fit by Nema et al. [47] is not accurate for low temperatures. The quadratic form of Eq. (2) is more reliable for the whole temperature range.

The intersection of the equilibrium curves for systems containing carbon dioxide results in a calculated quadrupole point of 271.70 K and 1042.67 kPa. These values are very close to those reported by Larson [38].

While the reliability of Eqs. (1) and (2) is apparent from the corresponding figures, their performance can be compared with other methods currently used to predict hydrate equilibrium pressure [66]. To assess the reliability of the models, the arithmetic average of the absolute values of relative errors (AARE%) can be used. It is defined as:

$$\text{AARE}\% = \frac{100}{N_d} \sum_{i=1}^{N_d} \left| \frac{P_i^{\text{exp}} - P_i^{\text{calc}}}{P_i^{\text{exp}}} \right| \quad (3)$$

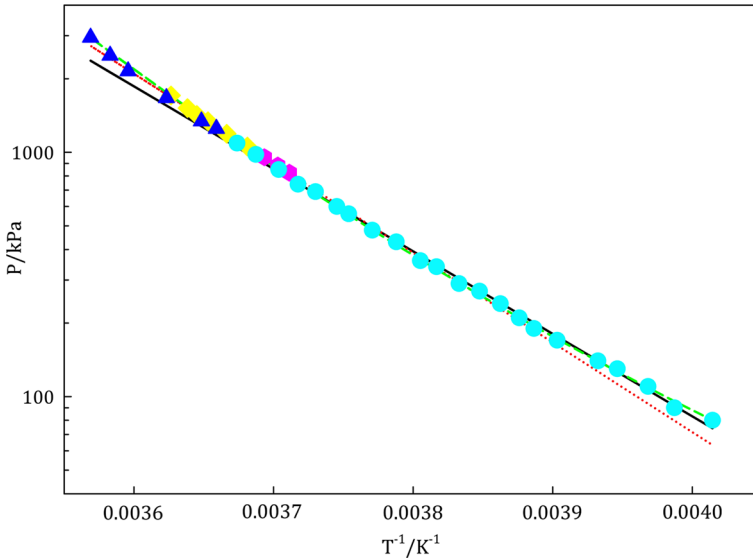


Fig. 8 Hydrate equilibrium pressure as a function of the reciprocal of temperature for carbon dioxide, supercooled water and hydrate: experimental data and modeling. (Melnikov et al. [46]: continuous line; Nema et al. [47]: dotted line; Eq. 2: dashed line; Nema et al. [47] water: filled diamond, Melnikov et al. [46] water: filled upward triangle; Nema et al. [47] supercooled water: empty square, Melnikov et al. [46] supercooled water: filled circle) (Color figure online)

A second measure of the reliability of the fitting procedure is the coefficient of determination R^2 , defined as:

$$R^2 = 1 - \frac{\sum_{i=1}^{N_d} (P_i^{\text{exp}} - P_i^{\text{calc}})^2}{\sum_{i=1}^{N_d} (\bar{P}^{\text{exp}} - P_i^{\text{calc}})^2} \quad (4)$$

A small value of AARE% and an R^2 value close to 1.0 denote a good correlation. Particularly, since the range of equilibrium pressures comprises data with different magnitude orders, the sum of absolute residuals (SAR) can also be used as a measure of fitting quality [67]. The value of SAR is sensitive to high-order data points (higher pressures). It is defined as:

$$\text{SAR} = \sum_{i=1}^{N_d} |P_i^{\text{exp}} - P_i^{\text{calc}}| \quad (5)$$

The value of SAR has a dimension of pressure and describes the reliability of the model for high-order data points.

Table 4 presents a comparison between the proposed equations and other well-known methods for the prediction/correlation of the equilibrium pressure of methane

Table 4 Comparison of different methods in the prediction/correlation of equilibrium pressure of methane, ice and hydrate

Method	AARE%	R^2	SAR (Pa)
Equation (1)	4.23	0.9987	978
Multiflash [19]	4.56	0.9987	1497
GERG & BS [16 and 15]	4.79	0.9985	1063
Anderson [62]	5.26	0.9986	898
PVTsim [18]	7.80	0.9949	1996
CSMHYD [21]	9.93	0.998	2260
CSMGem ^a [20]	4.02	0.9972	1395

^aDiverged at temperatures below 200 K (results are for 70% of data)

Table 5 Comparison of different methods in the prediction/correlation of equilibrium pressure of carbon dioxide, ice and hydrate

Method	AARE%	R^2	SAR (Pa)
Equation (1)	1.50	0.9992	332
Nema et al. [47]	1.95	0.9992	348
EOS-CG and BS [15, 17]	2.04	0.9992	501
Multiflash [19]	2.18	0.9992	481
Anderson [63]	2.38	0.9843	514
CSMGem [20]	6.76	0.9985	687
CSMHYD [21]	9.91	0.9990	1244
PVTsim [18]	21.6	0.9987	1333

vapor, ice and the corresponding hydrate. The experimental data by Delsemme and Wenger [27] were not considered in this calculation. The results for the equilibrium pressure of carbon dioxide, ice and hydrate are presented in Table 5.

Tables 4 and 5 show that proposed Eq. (1) is adequate to correlate the equilibrium data and allows calculations more precise than any other method, regardless of its complexity. The prediction of equilibrium pressure through highly accurate equations of states such as GERG-2008 [16] and EOS-CG [17] is the number one choice of iterative methods. The results of Multiflash [19] are more satisfactory in comparison with PVTsim [18] for both hydrates. The performance of CSMGem [20] is better than CSMHYD [21]. However, considering the necessity of a reasonable initial guess for the calculation, it easily fails to calculate the equilibrium pressure at low temperatures.

These methods can be used “in reverse,” i.e., to calculate the equilibrium temperature from the corresponding pressure. The corresponding AARE% is compared in Fig. 9 both for calculating the equilibrium pressure, AARE%_P, and for calculating the equilibrium temperature, AARE%_T. Due to the logarithm relationship, deviations in temperature are one magnitude order lower than pressure deviations. In any case, the calculations using Eq. (1) result in better agreement with the experimental data than

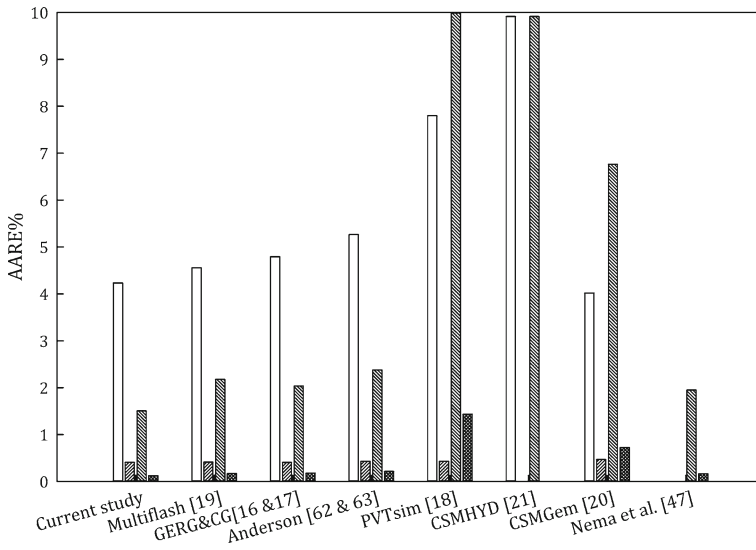


Fig. 9 Bar chart of the arithmetic average of the absolute values of the relative errors in the estimation of equilibrium pressure as a function of temperature and vice versa for different calculation methods. (AARE% methane: empty square; AARE_T% methane: square with upper right to lower left fill; AARE_P% carbon dioxide: square with upper left to lower right fill; AARE_T% carbon dioxide: square with diagonal crosshatch fill). Results for CSMGem are based on 70% of data (Color figure online)

Table 6 AARE% for the prediction of the equilibrium pressure of methane or carbon dioxide vapor, hydrate and supercooled water

Method	System	AARE%
Equation (1)	Methane/hydrate/supercooled water	1.62
Melnikov et al. [37]		1.75
Equation (2)	Carbon dioxide/hydrate/supercooled water	1.78
Melnikov et al. [46]		2.95
Nema et al. [47]		4.74

any other method. For the PVTsim method [18], the equilibrium temperature could not be calculated for pressures below 110 kPa for methane hydrates.

Finally, Table 6 presents the values of AARE% for the prediction and correlation of equilibrium pressure and temperature of methane or carbon dioxide vapor and hydrate and supercooled water. Once again, the results of the proposed equations are superior to those obtained by other methods.

3.2 Enthalpy Change of Hydrate Formation

The slope of the equilibrium pressure curve as a function of temperature is related to the enthalpy and volume change of any phase transition [68] through the Clapeyron equation [23]:

$$\frac{dP}{dT} = \frac{\Delta H}{T \Delta V} \quad (6)$$

A reasonable approximation is to consider the volume change equal to the volume of the vapor in the equilibrium, which leads to the Clausius–Clapeyron [24] equation:

$$\frac{d \ln(P)}{d(1/T)} = -\frac{\Delta H}{ZR} \quad (7)$$

The reliability of applying this equation to this equilibrium has been challenged by researchers [63, 64] mainly because it ignores the amount of vapor dissolved in the water of equilibria. To provide a better insight into this issue, we calculated the solubility of methane and carbon dioxide along equilibrium lines with ice and with supercooled water. For the methane–water system, the equation of state GERG-2008 [16, 69] was used, and for the carbon dioxide–water system, the equation of state of EOS-CG [17, 70] was used. The mole fraction of carbon dioxide dissolved in water is two magnitude orders higher than the mole fraction of methane under analogous conditions. However, even the solubility of carbon dioxide is very low—at the experimental conditions, the maximum value corresponds to a mole fraction less than 0.01.

Using the compressibility factors of methane and carbon dioxide calculated from Setzmann and Wagner [71] and Span and Wagner [72], the enthalpy change can be estimated through the Clausius–Clapeyron [24] equation. Figures 10 and 11 depict the result of current approach in comparison with values obtained from other methods for systems containing methane [62, 73–75] and carbon dioxide [63, 73, 76], respectively. For both cases, values are rather scattered: While some concordance among experimental and calculated values does exist, it is not perfect. For example, considering the equilibrium with methane, the experimental datum by Handa [74] falls exactly on the calculated line, while the experimental datum by Rydzy et al. [76] lies far from this line. Other calculated values, such as Yoon et al. [73], Avlonitis [75] and Anderson [62], are rather scattered, without a definite trend. A similar analysis can be carried out with the enthalpy of carbon dioxide hydrate formation. Calculation results by Yoon et al. [73] and Avlonitis [75] are close to the calculated ones, opposite to the results by Anderson [63].

The hydration number of hydrate can be estimated from the difference of enthalpy of hydrate dissociation in equilibrium with supercooled water and ice divided by the fusion enthalpy of water [77] at the quadruple point.

$$n = \left(\frac{\Delta H_{\text{supercooled water}}^{\text{hydrate}} - \Delta H_{\text{ice}}^{\text{hydrate}}}{\Delta H_{\text{liquid water}}^{\text{ice}}} \right)_{\text{@quadruple point}} \quad (8)$$

The estimated values of hydration numbers are 5.7 and 8.0 for methane [78] and carbon dioxide [79]. These values are close to known values, which shows that the estimative provided by the proposed equations is reasonable.

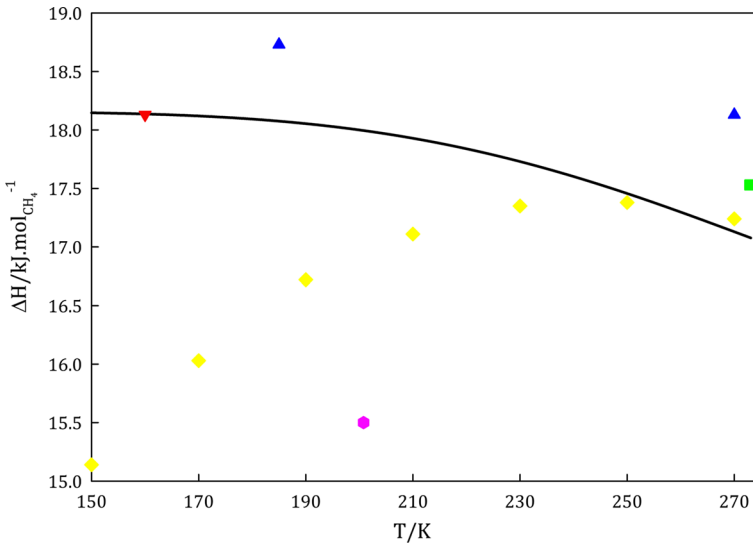


Fig. 10 Enthalpy of hydrate formation for hydrates containing methane. (This study: continuous line; Handa [74]: filled downward triangle; Yoon et al. [73]: filled square; Anderson [62]: filled diamond; Avlonitis [75]: filled upward triangle; Rydzy et al. [76]: empty square) (Color figure online)

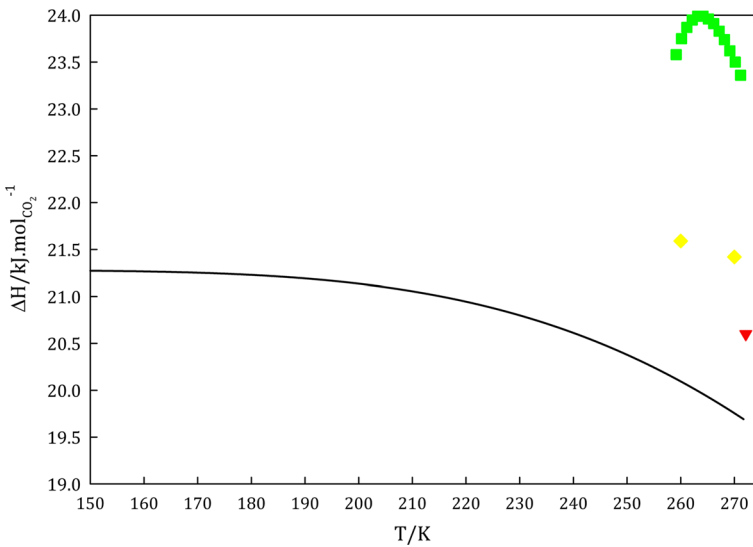


Fig. 11 Enthalpy of hydrate formation for hydrates containing carbon dioxide. (This study: continuous line; Yoon et al. [73]: filled upward triangle; Anderson [63]: filled square; Avlonitis [75]: filled diamond) (Color figure online)

4 Conclusion

Equilibrium literature data of methane and carbon dioxide hydrates at low temperatures have been reviewed. Constants of Arrhenius-type equation accurately determined for the mentioned equilibrium lines which allow calculating the hydrate equilibrium pressure at any temperature below the quadruple point for both systems contain ice and supercooled water. Through intersection analysis, new accurate quadruple points were determined. Interpretations based on flash calculations by high accurate equations of states shown enthalpies of clathrate formation/dissociation, for equilibrium below quadruple point, lead to the similarity of Clapeyron and Clausius–Clapeyron approaches. Based on equality of equilibrium conditions at the quadruple point, new hydration numbers were calculated. Gamma–phi approach through high accurate equations of states of GERG-2008 and CG for the prediction of VHIw three-phase equilibrium line was evaluated. Commercial packages of Multiflash and PVTsim and open-source codes of CSMGem and CSMHYD were used to model the phenomena.

Acknowledgements The authors appreciate the financial support of FAPESP (processes 2014/02140-7, 2014/25740-0, 2016/09341-3 and 2017/22589-7) and CNPq.

References

1. E.D. Sloan Jr., C. Koh, *Clathrate Hydrates of Natural Gases* (CRC Press, Boca Raton, 2007)
2. U. Hiroki, H. Akiba, S. Akatsu, R. Ohmura, *New J. Chem.* **39**, 8254–8262 (2015)
3. J.M. Brooks, H.B. Cox, W.R. Bryant, M.C. Kennicutt, R.G. Mann, T.J. McDonald, *Org. Geochem.* **10**, 221–234 (1986)
4. M. Kastner, K.A. Kvenvolden, T.D. Lorenson, *Earth Planet. Sci. Lett.* **156**, 173–183 (1998)
5. O. Mousis, J.L. Lunine, K.E. Mandt, E. Schindhelm, H.A. Weaver, S.A. Stern, J.H. Waite, R. Gladstone, A. Moudens, *Icarus* **225**, 856–861 (2013)
6. D. Ambuehl, M.E. Madden, *Icarus* **234**, 45–52 (2014)
7. R. Llopis, E. Torrella, R. Cabello, D. Sanchez, *Int. J. Refrig.* **35**, 810–816 (2012)
8. A. McCulloch, *J. Fluor. Chem.* **123**, 21–29 (2003)
9. W. Wu, B. Wong, W. Shi, X. Li, *Renew. Sustain. Energy Rev.* **31**, 681–707 (2014)
10. J. Javanmardi, Kh Nasrifar, S.H. Najibi, M. Moshfeghian, *Appl. Therm. Eng.* **25**, 1708–1723 (2005)
11. Z.R. Chong, S.H.B. Yang, P. Babu, P. Linga, X.S. Li, *Appl. Energy* **162**, 1633–1652 (2016)
12. R.H. James, P. Bousquet, I. Bussmann, M. Haeckel, R. Kipfer, I. Leifer, H. Niemann, I. Ostrovsky, J. Piskozub, G. Rehder, T. Treude, *Limnol. Oceanogr.* **61**, S283–S299 (2016)
13. C. Hope, K. Schaefer, *Nat. Clim. Change* **6**, 56–59 (2016)
14. J.H. van der Waals, J.C. Platteeuw, *Adv. Chem. Phys.* **2**, 1–57 (1959)
15. A.L. Ballard, E.D. Sloan Jr., *Fluid Phase Equilib.* **194**, 371–383 (2002)
16. O. Kunz, W. Wagner, *J. Chem. Eng. Data* **57**, 3032–3091 (2012)
17. J. Gernert, R. Span, *J. Chem. Thermodyn.* **93**, 274–293 (2016)
18. Calsep, Method documentation PVTsim 20, Calsep product (2011)
19. Infochem, *User guide for multiflash models and physical properties* (Infochem Computer Services Ltd., London, 2015)
20. A.L. Ballard, E.D. Sloan, *Fluid Phase Equilib.* **218**, 15–31 (2004)
21. http://hydrates.mines.edu/CHR/Software_files/CSMHYd.zip. (1998)
22. S. Arrhenius, *Z. Phys. Chem.* **4**, 96–116 (1889)
23. M.C. Clapeyron, *Journal de l'École polytechnique* **23**, 153–190 (1834)
24. R. Clausius, *Ann. Phys.* **155**, 368–397 (1850)
25. O.L. Roberts, E.R. Brownscombe, L.S. Howe, *Oil Gas J.* **39**, 37–43 (1940)

26. W.M. Deaton, E.M. Frost, *Gas Hydrates and Their Relation to the Operation of Natural-Gas Pipe Lines*, vol. 8, Monograph (United States Bureau of Mines, American Gas Association, Washington, 1946)
27. A.H. Delsemme, A. Wenger, *Planet. Space Sci.* **18**, 709–715 (1970)
28. B.J. Falabella, M. Vanpee, *Ind. Eng. Chem. Fundam.* **13**, 228–231 (1974)
29. T.Y. Makogon, E.D. Sloan Jr., *J. Chem. Eng. Data* **39**, 351–353 (1994)
30. S.O. Yang, Measurements and predictions of phase equilibria for water + natural gas components in hydrate-forming conditions. Ph.D. Dissertation, Korea University (2000)
31. A. Hachikubo, A. Miyamoto, K. Hyakutake, K. Abe, H. Shoji, in: Y.H. Mori (ed.), *Proceedings of Fourth International Conference on Gas Hydrates, Yokohama* (2002)
32. K. Yasuda, R. Ohmura, *J. Chem. Eng. Data* **53**, 2182–2188 (2008)
33. A.H. Mohammadi, D. Richon, *Ind. Eng. Chem. Res.* **49**, 3976–3979 (2010)
34. N. Fray, U. Marboeuf, O. Brissaud, B. Schmitt, *J. Chem. Eng. Data* **55**, 5101–5108 (2010)
35. H.D. Nagashima, R. Ohmura, *J. Chem. Thermodyn.* **102**, 252–256 (2016)
36. V.A. Istomin, V.G. Kwon, V.A. Durov, *Gas Ind. Rus.* **4**, 13–15 (2006)
37. V.P. Melnikov, A.N. Nesterov, A.M. Reshetnikov, A.G. Zavadovsky, *Chem. Eng. Sci.* **64**, 1160–1166 (2009)
38. S.D. Larson, Phase studies of the two-component carbon dioxide-water system, involving the carbon dioxide hydrate. Ph.D. Dissertation, University of Illinois (1955)
39. S.L. Miller, W.D. Smythe, *Science* **170**, 531–533 (1970)
40. A.W. Adamson, B.R. Jones, *J. Colloid Interface Sci.* **37**, 831–835 (1971)
41. B.J. Falabella, A study of natural gas hydrates. Ph.D. Dissertation, University of Massachusetts, 1975
42. B. Schmitt, La surface de la glace: structure, dynamique et interactions—implications astrophysique. Ph.D. Dissertation, University of Grenoble (1986)
43. M. Wendland, H. Hasse, G. Maurer, *J. Chem. Eng. Data* **44**, 901–906 (1999)
44. A.H. Mohammadi, D. Richon, *J. Chem. Eng. Data* **54**, 279–281 (2009)
45. H.D. Nagashima, N. Fukushima, R. Ohmura, *Fluid Phase Equilib.* **413**, 53–56 (2016)
46. V.P. Melnikov, A.N. Nesterov, A.M. Reshetnikov, V.A. Istomin, *Chem. Eng. Sci.* **66**, 73–77 (2010)
47. Y. Nema, R. Ohmura, I. Senaha, K. Yasuda, *Fluid Phase Equilib.* **441**, 49–53 (2017)
48. G.J. Chen, T.M. Guo, *Chem. Eng. J.* **71**, 145–151 (1998)
49. I. Langmuir, *J. Am. Chem. Soc.* **30**, 1361–1403 (1918)
50. I.V. Yakoumis, G.M. Kontogeorgis, E.C. Voutsas, E.M. Hendriks, D.P. Tassios, *Ind. Eng. Chem. Res.* **37**, 4175–4182 (1998)
51. A. Martín, *J. Phys. Chem. B* **114**, 9602–9607 (2010)
52. A. Asiaee, S. Raeissi, A. Shariati, *J. Chem. Thermodyn.* **43**, 822–827 (2011)
53. I.N. Tsimpanogiannis, N.I. Papadimitriou, A.K. Stubos, *Mol. Phys.* **110**, 1213–1221 (2012)
54. W.R. Parrish, J.M. Prausnitz, *Ind. Eng. Chem. Proc. Des. Dev.* **11**, 26–35 (1972)
55. G.D. Holder, G. Corbin, K.D. Papadopoulos, *Ind. Eng. Chem. Fundam.* **19**, 282–286 (1980)
56. J.B. Klauda, S.I. Sandler, *Ind. Eng. Chem. Res.* **39**, 3377–3386 (2000)
57. S.Y. Lee, G.D. Holder, *AIChE J.* **48**, 161–167 (2002)
58. J.B. Klauda, S.I. Sandler, *Chem. Eng. Sci.* **58**, 27–41 (2003)
59. A.A. Bandyopadhyay, J.B. Klauda, *Ind. Eng. Chem. Res.* **50**, 148–157 (2011)
60. G. Soave, *Chem. Eng. Sci.* **27**, 1197–1203 (1972)
61. V. Vinš, A. Jäger, J. Hrubý, R. Span, *Fluid Phase Equilib.* **435**, 104–117 (2017)
62. G.K. Anderson, *J. Chem. Thermodyn.* **36**, 1119–1127 (2004)
63. G.K. Anderson, *J. Chem. Thermodyn.* **35**, 1171–1183 (2003)
64. G. Armstrong, *Nat. Chem.* **2**, 256 (2010)
65. M.S. Selim, E.D. Sloan, *AIChE J.* **35**, 1049–1052 (1989)
66. A. Jarrhian, E. Heidaryan, *J. Nat. Gas Sci. Eng.* **20**, 50–57 (2014)
67. E. Heidaryan, A. Jarrhian, *Can. J. Chem. Eng.* **91**, 1183–1189 (2013)
68. H.-J. Ng, D.B. Robinson, *AIChE J.* **23**, 477–482 (1977)
69. E.W. Lemmon, M.L. Huber, M.O. McLinden, NIST reference fluid thermodynamic and transport properties—REFPROP 9.1 (2013)
70. R. Span, T. Eckermann, S. Herrig, S. Hielscher, A. Jäger, M. Thol, Thermodynamic reference and engineering data—TREND 3.0 (2016)
71. U. Setzmann, W. Wagner, *J. Phys. Chem. Ref. Data* **20**, 1061–1155 (1991)
72. R. Span, W. Wagner, *J. Phys. Chem. Ref. Data* **25**, 1509–1596 (1996)

73. J.H. Yoon, Y. Yamamoto, T. Komai, H. Haneda, T. Kawamura, *Ind. Eng. Chem. Res.* **42**, 1111–1114 (2003)
74. Y.P. Handa, *J. Chem. Thermodyn.* **18**, 915–921 (1986)
75. D. Avlonitis, *AIChE J.* **51**, 258–1273 (2005)
76. M.B. Rydzy, J.M. Schicks, R. Naumann, J. Erzinger, *J. Phys. Chem. B* **111**, 9539–9545 (2007)
77. R. Feistel, W. Wagner, *J. Phys. Chem. Ref. Data* **35**, 1021–1047 (2006)
78. A. Gupta, J. Lachance, E.D. Sloan, C.A. Koh, *Chem. Eng. Sci.* **63**, 5848–5853 (2008)
79. T. Uchida, *Waste Manage.* **17**, 343–352 (1998)